



The influence of landscape spatial configuration on nitrogen and phosphorus exports in agricultural catchments

Antoine Casquin · Rémi Dupas · Sen Gu · Ewan Couic · Gérard Gruau · Patrick Durand

Received: 17 February 2021 / Accepted: 23 July 2021 / Published online: 21 August 2021
© The Author(s), under exclusive licence to Springer Nature B.V. 2021

Abstract

Context Nitrogen (N) and phosphorus (P) exports from rural landscapes can cause eutrophication of inland and coastal waters. Few studies have investigated the influence of the spatial configuration of nutrient sources—i.e. the spatial arrangement of agricultural fields in headwater catchments—on N and P exports.

Objectives This study aimed to (1) assess the influence of the spatial configuration of nutrient sources on nitrate (NO_3^-) and total phosphorus (TP) exports at the catchment scale, and (2) investigate how relationships between landscape composition (% agricultural land-use) and landscape configuration vary depending on catchment size.

Methods We analysed NO_3^- and TP in 19 headwaters (1–14 km², Western France) every two weeks for 17 months. The headwater catchments had similar soil types, climate, and farming systems but differed in landscape composition and spatial configuration. We developed a landscape configuration index (LCI) describing the spatial organisation of nutrient sources as a function of their hydrological distance to streams and flow accumulation zones. We calibrated the LCI's two parameters to maximise the rank correlation with median concentrations of TP and NO_3^- .

Results We found that landscape composition controlled NO_3^- exports, whereas landscape configuration controlled TP exports. For a given landscape composition, landscape spatial configuration was highly heterogeneous at small scales (< 10 km²) but became homogeneous at larger scales (> 50 km²).

Supplementary Information The online version contains supplementary material available at <https://doi.org/10.1007/s10980-021-01308-5>.

A. Casquin (✉) · R. Dupas · P. Durand
INRAE, UMR SAS 1069, L'Institut Agro, 65 Rue de St
Brieuc, 35200 Rennes, France
e-mail: a.casquin@gmail.com

R. Dupas
e-mail: remi.dupas@inrae.fr

P. Durand
e-mail: patrick.durand@inrae.fr

S. Gu · E. Couic · G. Gruau
OSUR, Géosciences Rennes, CNRS, UMR 6118, Campus
de Beaulieu, 35042 Rennes, France
e-mail: gusen@ihb.ac.cn

E. Couic
e-mail: ewan.couic@univ-rennes1.fr

G. Gruau
e-mail: gerard.gruau@univ-rennes1.fr

S. Gu
Institute of Hydrobiology, Chinese Academy of Sciences,
Wuhan 430072, China

Conclusions The spatial configuration of nutrient sources influences TP but not NO_3^- exports. An ideal placement of mitigation measures to limit diffuse TP export should consider both the hydrological distance to streams and flow accumulation zones.

Keywords Eutrophication · Landscape pattern · Landscape organisation · Landscape composition · Heterogeneity · Scaling

Introduction

Excessive loads of nitrogen (N) and phosphorus (P) cause the eutrophication of marine and freshwater ecosystems (Dodds and Smith 2016; Le Moal et al. 2018), which threatens biodiversity and human activities (Steffen et al. 2015). In streams and rivers that drain agricultural landscapes, N and P originate mainly from fertilised agricultural fields. Water quality mitigation measures such as set-aside areas, buffer zones or cover crops often result in reduced yields or increased production costs; hence, they decrease profitability for farmers (Withers et al. 2014). It is therefore necessary to locate mitigation options where they will be most effective (Cole et al. 2020). Mechanistic models (McDowell et al. 2014; Casal et al. 2019) and methods based on statistical analysis of landscape properties (Doody et al. 2012; Hashemi et al. 2018) have been used to optimise locations of mitigation practices.

Most N and P enter the hydrographic network in headwater streams (Dodds and Oakes 2008), which represent 90% of global stream length (Downing 2012) but are rarely monitored, except for research purposes (Bishop et al. 2008). At this scale, nutrient exports vary greatly in space (Temnerud and Bishop 2005; Abbott et al. 2018). While in large ($> 100 \text{ km}^2$) catchments, both N and P exports can be statistically related to proxies of agricultural pressure, such as percentage of agricultural land-use or agricultural surplus (Dupas et al. 2015; Goyette et al. 2018), these relationships break down at the scale of headwater catchments ($< 20 \text{ km}^2$) (Burt and Pinay 2005; Bol et al. 2018). The reason why the relationship between landscape composition (percentage of agricultural land-use) and nutrient exports is scale-dependent is unclear. Identifying the factor(s) responsible for this

loss of relationship, and the characteristic spatial scale at which it occurs, would help guide water quality mitigation measures at the catchment scale. In this article, we explore the hypothesis that the spatial configuration of nutrient sources—i.e. the spatial arrangement/distribution/organisation of agricultural fields, hereafter called “landscape configuration”,—influences N and P exports at the headwater catchment scale. For a given region, landscape spatial configuration can be highly heterogeneous among headwater catchments but homogeneous among larger catchments (Temnerud and Bishop 2005; Abbott et al. 2018). If verified, these two hypotheses could explain the breakdown of the relationship between agricultural pressure and nutrient exports at the headwater catchment scale.

Several authors have reviewed the influence of landscape spatial configuration on nutrient loads at multiple scales (Uuemaa et al. 2007; Lintern et al. 2018). Metrics used in landscape ecology are based on the area/density/edge, shape, isolation, interspersion, and connectivity of patches, and they have been applied to predict water quality parameters at the catchment scale (Shi et al. 2013; Xiao et al. 2016; Liu et al. 2020). However, these approaches often rely on regressions of several landscape metrics and water quality parameters, which risks over-fitting certain relationships and/or spurious correlations. Landscape spatial configuration can also be viewed as the overlap and proximity of features such as streams, depressions, and flow accumulation areas to land-use patches (e.g. crops, forest fragments, urban fabric). In line with this concept, Peterson et al. (2011) related parameters of stream ecological conditions to multiple spatially explicit landscape “topological” metrics and found that these spatially explicit methods clearly had more predictive power than landscape composition metrics. Staponites et al. (2019), using similar metrics, suggested that the spatial organisation of nutrient sources (i.e. landscape configuration) influenced the transfer of reactive or labile water quality parameters (e.g. total phosphorus (TP), orthophosphate⁻ and nitrite), whereas percentages of land use (i.e. landscape composition) have more predictive power for more temporally stable water quality parameters [e.g. calcium, nitrate (NO_3^-), conductivity]. These results are consistent with current knowledge on transfer pathways of nutrients in catchments, with deeper flowpaths for N species than for P species (Strohmeier et al.

2020), and explains why landscape features had less influence on NO_3^- than P (Thomas and Abbott 2018). These landscape metrics, however, are relatively rigid, as topological influences (e.g. hydraulic distance to stream, surface flow accumulation, slope), whether considered in the metrics or not, cannot be weighted. In addition, certain topological features vary over a much wider range of values than others, which may obscure other features when no weighting coefficient is included in the landscape metric. For example, flow accumulation (which can have large values) can overshadow the influence of slope (which varies over a narrow range of values) in an index that considers both without weighting them.

The idea that landscape configuration influences N and P loads is the basis for the concept of critical source area (CSA), i.e. the idea that a small percentage of the agricultural area (e.g. <20% of the agricultural area within a catchment) contributes disproportionately to the nutrients transferred to streams (e.g. >80% of the load)—CSAs are defined as the intersection of nutrient sources and hydrologically sensitive areas (Gburek and Sharpley 1998; Pionke et al. 2000). Initially defined at the sub-field scale, the concept of CSA was extended to larger scales; entire fields or subcatchments can also be classified as CSAs (Page et al. 2005; Srinivasan and McDowell 2009; Sharpley et al. 2011; Buchanan et al. 2013b; Reaney et al. 2019). Substantial uncertainties remain, however, in their delineation at all scales (Doody et al. 2012). Validation at the sub-field scale can be based on observing erosion marks (Reaney et al. 2019) or tracers (Collins et al. 2012). However, studies that validate CSA delineation based on N or P concentrations in streams and rivers are rare and are based on only a few hydrologically contrasting headwater catchments (McDowell and Srinivasan 2009; Shore et al. 2014; Thomas et al. 2016a) or larger catchments for which land-use composition is already a good predictor (Giri et al. 2018).

To address the limits of “expert-based” delineation of CSAs and the rigidity of spatially explicit landscape metrics, we developed a stochastic, data-driven approach based on 30 synoptic samplings of 19 agricultural headwater catchments to answer two questions: (i) Does landscape configuration influence N and P exports?; and (ii) Does the location of CSAs depend on the hydrological distance of the nutrient source to the hydrological network, their overlap with

flow accumulation areas, or both? We then investigated why some relationships between water quality parameters and landscape composition metrics break down below a certain catchment size. For this, we studied how the relationship between landscape composition and configuration varied as a function of catchment size in 500 randomly selected subcatchments in the study area.

Methods

Study site

The Yvel catchment is a 375 km² agricultural catchment of Strahler order 5 in Brittany, western France (Fig. 1). The Yvel River is the main tributary of a three million m³ water reservoir that has been subjected to cyanobacteria blooms since the 1970s (ODEM 2012), for which N and P are deemed responsible (Shatwell and Köhler 2018).

The climate is temperate oceanic with mean annual precipitation (1998–2017) of 777 mm (standard deviation, SD = 132 mm), mean annual temperature of 11.7 °C (SD = 0.5 °C), and mean annual runoff of 254 mm (SD = 143 mm). The Yvel River’s discharge is monitored for 300 km² of its 375 km² (Fig. 1), and monthly mean discharge at the DREAL station J8363110 varies from 0.16 m³s⁻¹ in August to 5.60 m³s⁻¹ in February. The low-flow season generally spans from July to October while the high-flow season spans from December to May, November and June being transition months. The hydrology is controlled by the dynamics of the shallow groundwater within unconsolidated weathered material that caps impervious schist bedrock (Casquin et al. 2020). The land use is dominated by arable fields (maize and winter cereals), which cover 54% of the catchment (Fig. 1). Grasslands (21%, mainly leys in rotation), forests (18%), and urban areas (6%) comprise the rest of the catchment area. Hedgerow density is 7.1 km km⁻². Soils in the catchment are generally shallow (< 100 cm), are well-drained in the upland part of the hillslope, and are often hydromorphic in valley bottoms. The elevation varies from 33 to 297 m above sea level. The centre of the catchment is the flattest area (most slopes < 5%), with long and regular hillslopes. In the north and south, the relief is more rugged, with shorter and steeper slopes. The southeast

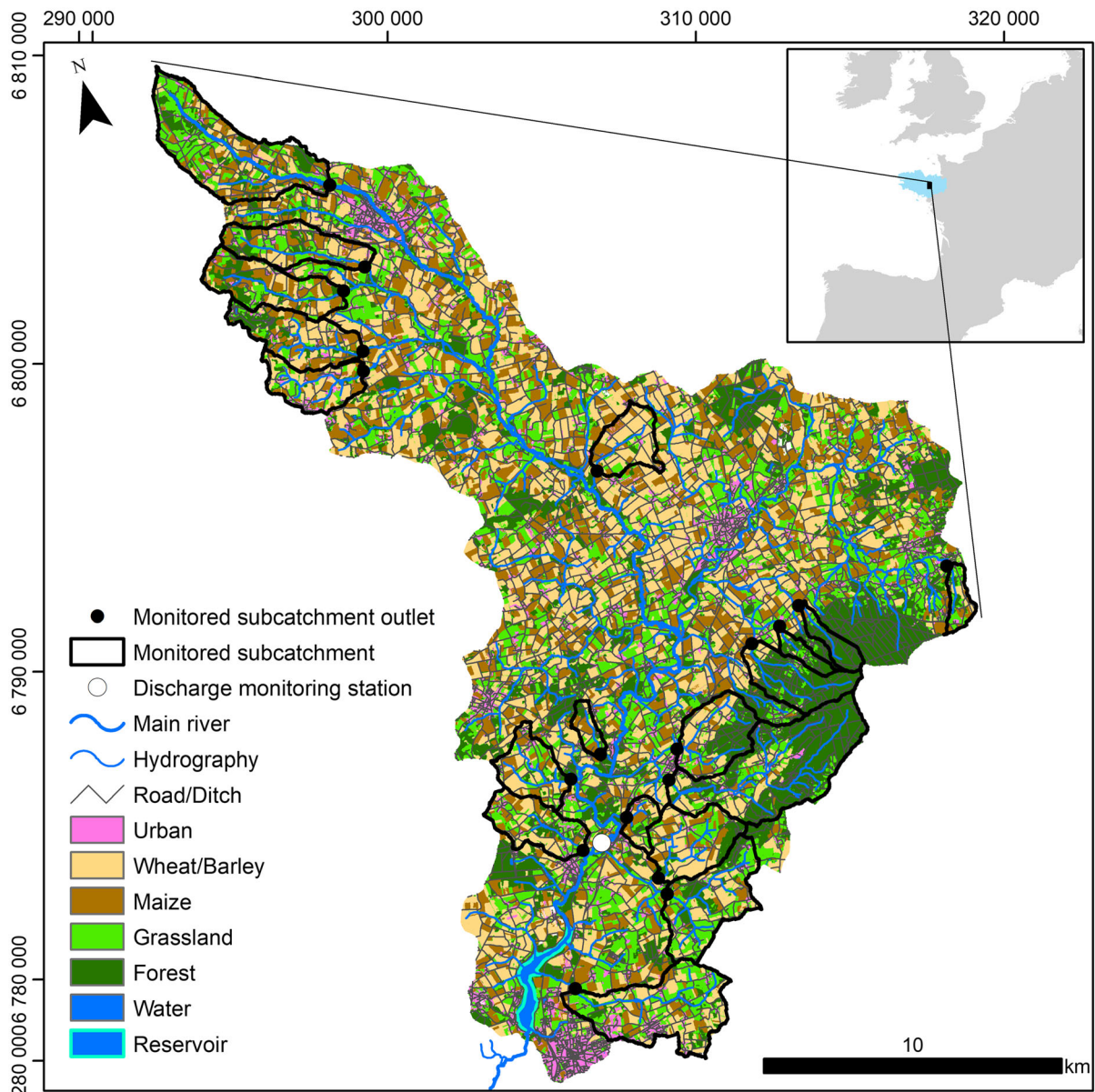


Fig. 1 Monitored subcatchments, land use in 2018, hydrography and roads/ditches in the Yvel catchment. The inset shows the location of Brittany, France, in western Europe

portion of the watershed of the catchment is forested and has the steepest slopes (5–15 %). A more detailed description of the study site can be found in Casquin et al. (2020).

Subcatchment monitoring

The monitoring strategy consisted of repeated synoptic sampling of 19 subcatchments (Fig. 1). The 19

subcatchments were selected based on Strahler order (1–2), size (0.8–12.6 km², mean = 5.1 km²), absence of a wastewater treatment plant, and accessibility. Their percentage of agricultural land-use ranged from 17 to 94% (mean = 74%), with mean slopes ranging from 2.7 to 6.6% (mean = 4.9%). Together, these 19 subcatchments covered 28% of the Yvel catchment's area. All 19 monitoring stations were sampled 30 times, approximately every two weeks from April

2018 to July 2019. Samples were filtered *in situ* immediately after sampling with cellulose acetate filters of 0.20 µm pore size for nitrate (NO₃⁻) analysis. All filters were rinsed in the laboratory with 20 ml of deionised water before use. An unfiltered water sample was also collected to analyse TP. The samples were transported to the laboratory in a cool box and then refrigerated at 4 °C until analysis. TP was analysed within 48 h of sampling, while NO₃⁻ was analysed within one week. TP was determined colorimetrically via reaction with ammonium molybdate (Murphy and Riley 1962) after digesting the samples in acidic potassium persulfate. The precision of TP measurements was ± 13 µg L⁻¹, while that of NO₃⁻ concentrations, analysed by ionic chromatography (Dionex, DX120), was ± 4 %. Previous work in the Brittany region showed that nitrate represented > 85 % of total N (Dupas et al. 2015). Hydrochemical data are available at <https://www.hydroshare.org/resource/7c7d7f6dd1f14450883ae1c243c3c28f/> (Dupas et al. 2020).

Spatial data sources and pre-processing

To investigate the influence of landscape configuration on N and P exports, we computed a landscape metric (see Sec. “[Landscape configuration index](#)”) that considers the hydrographic network, topography and nutrient sources.

Hydrographic network

The hydrographic network consisted of both the “natural” stream network and the ditch network because (1) it is often difficult to distinguish a ditch from a rectified stream and (2) our synoptic sampling verified that most of the ditches were deep (> 1 m) and were active in winter (high-flow season). Ditch networks are a shortcut between agricultural areas and the “natural” river network (Ahiablame et al. 2011; Buchanan et al. 2013a). Moreover, evidence suggests that ditches act as 1st order streams when considering nutrient spiralling and can retain and remobilise N and P (Dunne et al. 2007; Smith 2009; Hill and Robinson 2012). Thus, we considered them part of the hydrographic network. We used the road network as a proxy for the ditch network, as we observed that ditches bordered all roads in the study area. Streams (permanent and intermittent) and roads were extracted from

vector data (accuracy of ca. 1.5 m) provided by the *Institut National de l’Information Géographique et Forestière* (IGN) at 1:25,000 scale. We converted these vector data to raster format (spatial resolution of 10 m) and aligned them with the Digital Elevation Model (DEM) for later analysis.

Digital elevation model

The DEM, with a native resolution of 5 m (IGN 2018), was resampled to 10 m using cubic splines in ArcGIS 10.6 and was used as a reference layer for the rasterisation of the hydrographic network layer and nutrient sources layer. Filling was used to remove the depressions on hillslopes (Planchon and Darboux 2002), and the value “NA” was assigned to the pixels corresponding to roads and streams. We calculated flow accumulation and the hydrological distances to streams (i.e. following the surface flow paths) using the multiple flow direction algorithm (Qin et al. 2007). We chose this algorithm for its ability to generate realistic flow accumulation maps, unlike the D8 algorithm (O’Callaghan and Mark 1984).

Nutrient sources

We extracted the agricultural area data from the national land parcel identification system (Levasseur et al. 2016). The data are provided as a vector dataset at the 1:5000 scale for each year since 2010 and contain field boundaries and a code that identifies the crop type. We used the 2018 dataset and verified the spatial accuracy of the agricultural area boundaries based on 50 cm orthophotos and the hydrography. We then rasterized this dataset aligned with the DEM (spatial resolution of 10 m). We assigned the value 1 to agricultural areas and 0 to non-agricultural areas. We included riparian buffer strips in agricultural areas because they are recent and have been fertilised for years, and are a well-documented legacy source of nutrients in headwater catchments (Gu et al. 2018).

Landscape configuration index

We developed the landscape configuration index (LCI) (Eq. 1) to test the hypothesis that the hydrological proximity of agricultural areas to watercourses and their overlap with flow accumulation areas

influence nutrient exports at the headwater catchment scale. For each monitored subcatchment, the LCI was calculated as follows:

$$LCI(a, b) = \frac{\frac{1}{n} \times \sum_{i=1}^n LU_i \times FAcc_i^a \times FLS_i^{-b}}{\frac{1}{N} \times \sum_{i=1}^N LU_i \times FAcc_i^a \times FLS_i^{-b}} \quad (1)$$

where a and b are calibrated parameters, $i = 1 \dots n$ are the pixels of a subcatchment; $i = 1 \dots N$ are the pixels of the entire Yvel catchment, $FAcc_i$ is the flow accumulation on pixel i (m^2), FLS_i (m) is the distance along the surface flow line from pixel i to the stream/ditch, and LU_i equals 1 if pixel i is a source of nutrients (i.e. an agricultural area), otherwise 0.

Figure 2 Steps used to calculate the LCI given $a = 1.5$ and $b = 1.0$ for 2 of the 19 monitored subcatchments. Example of agricultural subcatchments with similar landscape composition [% agricultural area, proportional to LCI for $(a, b) = (0, 0)$] but contrasting landscape configuration [LCI values for $(a, b) \neq (0, 0)$]. a Denominator (Eq. 1) calculation steps for $a = 1.5$ and $b = 1$. b and c Numerator (Eq. 1) and LCI calculation steps for $a = 1.5$ and $b = 1$ in two monitored subcatchments. Pixel colour indicates the value of the pixel for the different terms of Eq. 1. Note the logarithmic colour scale, blank is NA.

The denominator is a normalisation factor that corresponds to the mean value of the numerator for the entire Yvel catchment. When $LCI > 1$, a subcatchment's nutrient sources are located predominantly in flow accumulation zones and/or near streams compared to the entire Yvel catchment.

By construction, when a and b equal 0 for a subcatchment, its LCI equals its percentage of agricultural land-use (i.e. the landscape composition) divided by the percentage of agricultural land-use in the entire Yvel catchment. For other values of a and b , the LCI indicates the landscape configuration. High values of parameter a increase the weight of pixels in flow accumulation zones in the LCI, while high values of parameter b increase the weight of pixels in near-stream zones.

Optimisation of (a, b) parameters and interpretation

We varied a and b to maximize Spearman's rank correlation (ρ) between the LCI and median NO_3^- and TP concentrations of the 19 monitored subcatchments

(Fig. 3). For large values of a or b , the LCI assigns high weights to a small percentage of the area. We restricted the ranges of parameters a and b so that a few pixels with the highest $FAcc$ and lowest FLS would not control the values of LCI. We explored the parameter space for pairs of (a, b) for which the sum of $FAcc_i^a \times FLS_i^{-b}$ in the top 5% pixels did not exceed 95% of the sum of $FAcc_i^a \times FLS_i^{-b}$ in all pixels in the Yvel catchment. We performed a systematic computation of the LCI in the 19 subcatchments, by sampling a and b every 0.1 from 0 to 2 for a and 0 to 4 for b . This led to 595 correlations computed (for NO_3^- and for TP), when excluding the cases when too few pixels determine the total value of the LCI.

Since several of the subcatchments were intermittent, we calculated the median concentrations for the 22 dates (out of 30) when at least 17 of the 19 subcatchments were flowing, so as not to bias calculation of the median concentrations. We focused on ranks rather than concentrations because several studies have shown that concentration estimates had high uncertainty when calculated with low-frequency data (e.g. Cassidy and Jordan 2011; Moatar et al. 2020), while the ranks of subcatchments could be predicted with high degree of confidence, as they are stable across flow conditions (Abbott et al. 2018; Dupas et al. 2019, Gu et al., 2021). The result interpretation was twofold:

- The spatial configuration of sources was considered to have an effect if ρ for at least one pair $(a, b) \neq (0, 0)$ was statistically significant ($p < 0.05$) and substantially higher (> 0.1) than that for $(a, b) = (0, 0)$.
- Optimal values of a and b were examined to assess the relative importance of hydrological distance to streams and flow accumulation on hillslopes.

Scaling of the optimized LCI

In order to verify the hypothesis that landscape configuration can be highly heterogeneous at small scales among subcatchments but homogeneous among larger subcatchments, we calculated the optimized LCI at the field scale, in 1 and 25 km^2 subcatchments of the study area. We then calculated the ratio of LCI with optimal (a, b) (landscape configuration) to LCI with $(a, b) = (0, 0)$ (landscape composition) for 500 randomly generated subcatchments (range: 0.5–375

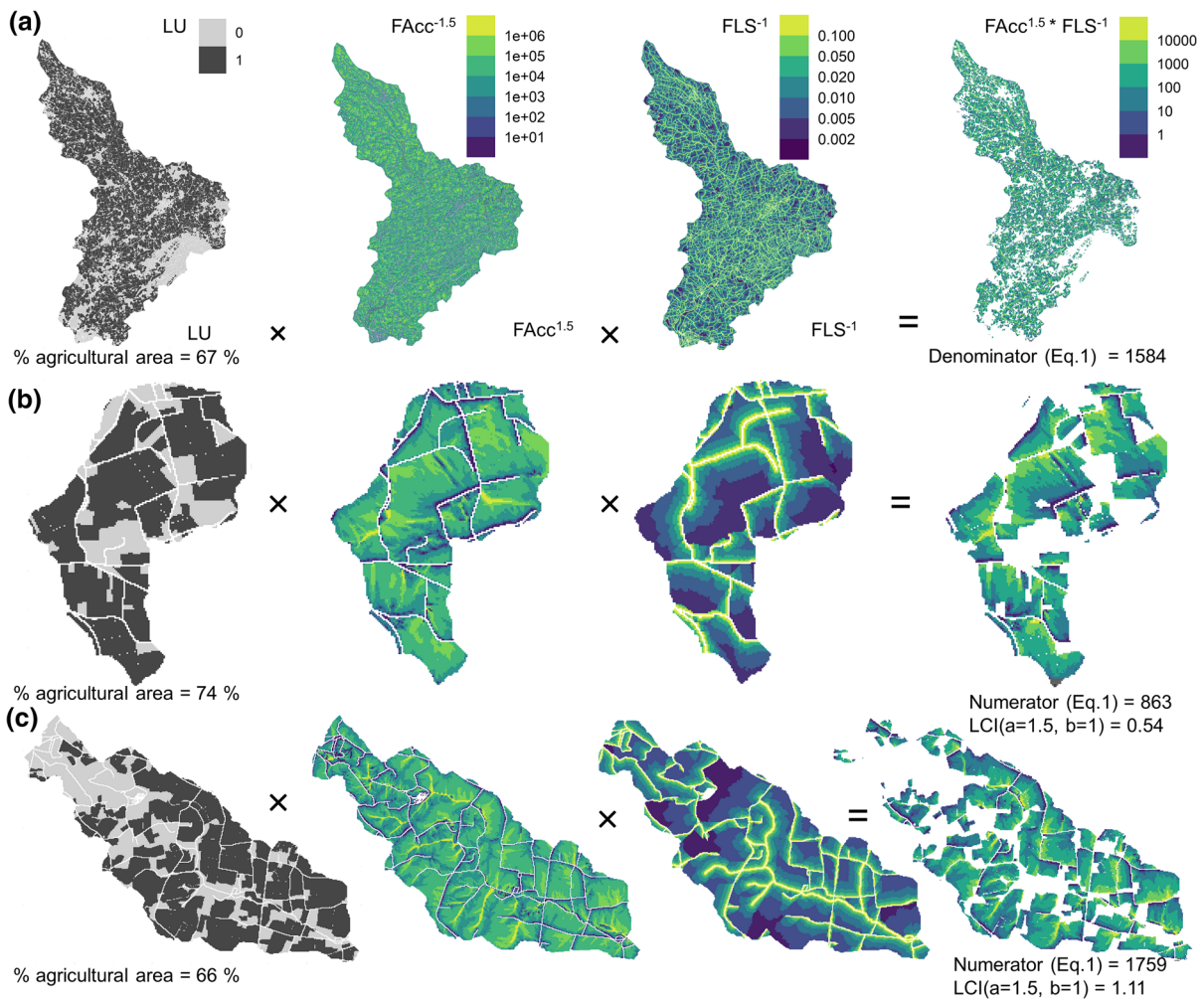


Fig. 2 presents a detailed calculations for two subcatchments with similar land-use composition, but whose LCI varies by a factor of 2 when parameters (a, b) = (1.5, 1)

km²) in the Yvel catchment. Finally, we analysed how the relationship between these two metrics evolved as catchment size increased.

Results

Comparison of land-use composition and configuration metrics as predictors of NO₃⁻ and TP concentrations in headwater catchments

Landscape composition [i.e. LCI with (a, b) = (0, 0)] predicted median NO₃⁻ concentrations well (ρ = 0.84, p < 0.05) but not those of TP (ρ = 0.33, p > 0.05). Varying (a, b) did not substantially

improved (maximum ρ = 0.86, for a = 0.1 and b = 0) the prediction of median NO₃⁻ concentration rank; thus, landscape composition predicted NO₃⁻ exports well at the headwater catchment scale, and considering landscape configuration did not improve the prediction (Fig. 3a). For NO₃⁻, this result refutes our first hypothesis that the spatial configuration of nutrient sources influences nutrient exports.

The correlation between the percentage of agricultural land and median TP concentrations [(a, b) = (0, 0)] was 0.35 (ρ = 0.15, p > 0.05) (Fig. 3b). This correlation improved as weights increased for sources near streams (ρ increased as b increased) and for sources that overlapped surface flow accumulation (ρ increased as a increased) (Fig. 3a). This confirms our

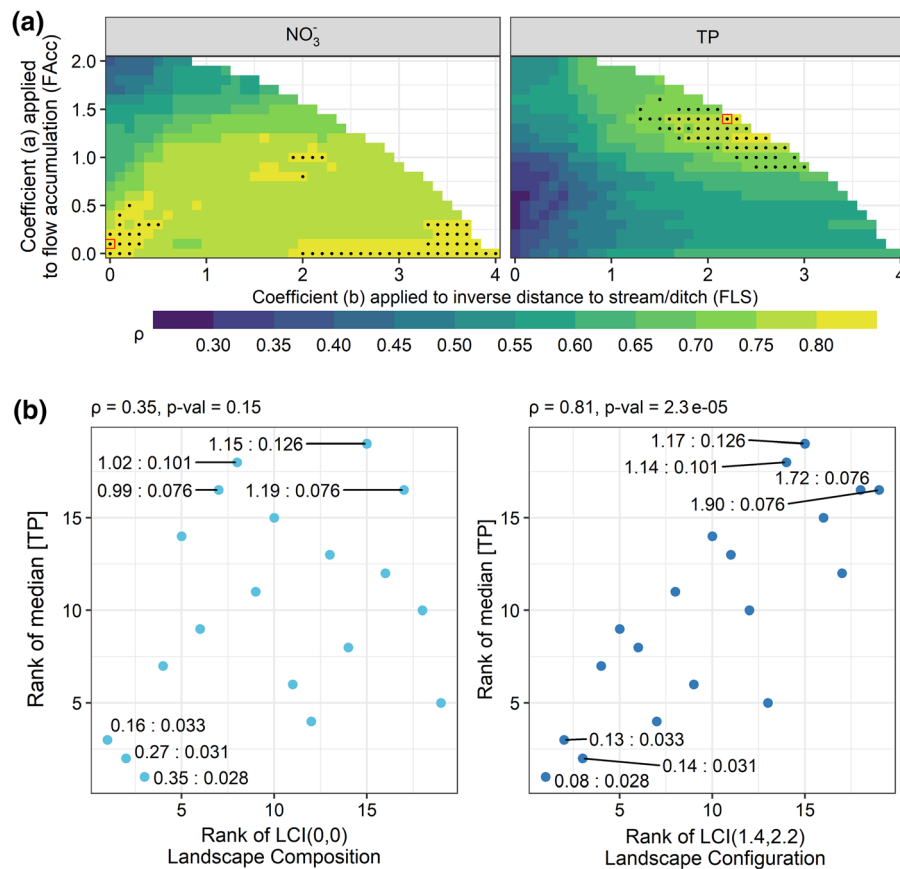


Fig. 3 a Optimisation plans for LCI parameters a and b used to predict median concentration of NO_3^- and TP in 19 headwater catchments. Rank correlations (ρ) not shown (blank) indicate (a, b) outside of the exploration domain. For each optimisation plan, black dots indicate 10% highest ρ , red square the best

correlation b Scatter plots between ranks of median [TP] and ranks of landscape composition (left) and optimised LCI for TP (right). Each point represents a monitored subcatchment. Annotations show LCI(a, b) values:median [TP] values

first hypothesis that landscape configuration influences P exports, and agricultural areas near watercourses and that overlap surface flow accumulation areas result in larger P exports. The optimum correlation was obtained for $a = 1.4$ and $b = 2.2$ ($\rho = 0.81$, $p = 2.2 \times 10^{-5}$, $p < 0.05$), at the limit of the exploration domain for (a,b), which means that 5% of the area determined nearly 95% of the LCI.

Using the same parameter exploration scheme, we optimised (a, b) for TP concentrations on each sampling date (Fig. 4c). The LCI with (a, b) \neq (0, 0) always predicted TP concentrations better than landscape composition (Fig. 4a). The correlation between the optimised LCI and TP concentrations differed significantly ($p < 0.05$) from 0 for all but one sampling date, except during the low-flow periods (Fig. 4b).

During the low-flow season (Aug–Nov 2018, Jul 2019) and beginning of the rewetting season (Nov 2018), TP concentrations in the headwaters did not correlate with the optimised LCI ($p > 0.05$) (Fig. 4b). Note that 13 of the 19 streams were dry at the peak of the low-flow season. Outside the low-flow season, optimal values of parameters a and b were stable, varying little around a median value of 1.4 and 2.2, respectively. Therefore, the total weight of the top 5% of weighted area remained close to 95% (Fig. 4d), except during the low-flow season. The optimised LCI based on median TP concentrations, hereafter referred to as LCI-TP, appears to be a robust sensitivity index to determine TP CSAs across flow conditions.

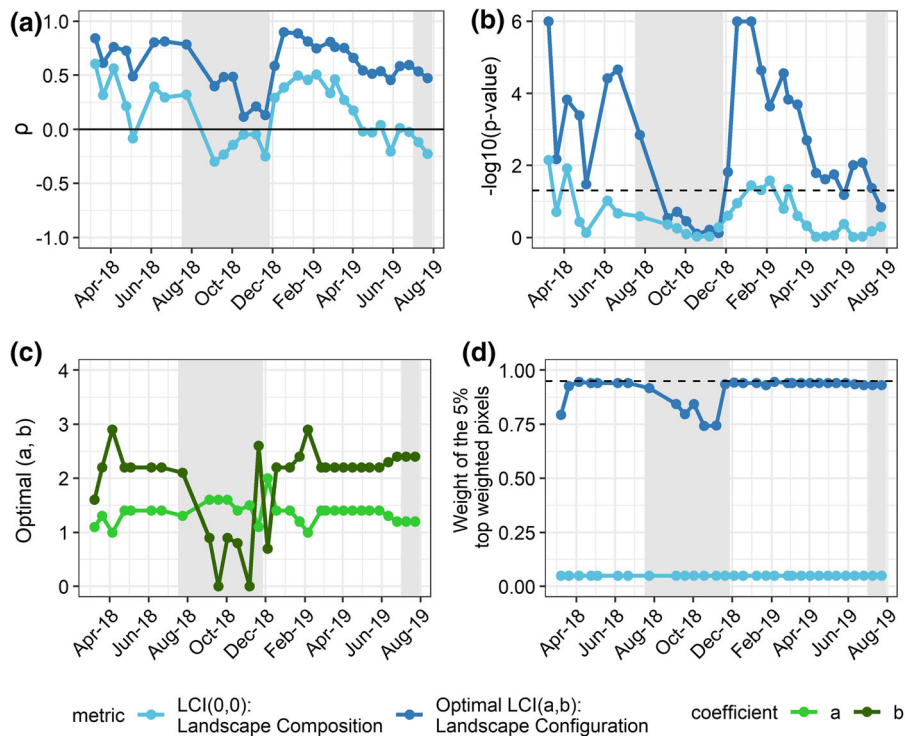


Fig. 4 Comparison of landscape composition and optimised LCI as predictors of TP concentrations, for all sampling dates. **a** Spearman's rank correlation (ρ), **b** associated $-\log_{10}$ -transformed p values, dashed line indicates $p = 0.05$, points above indicates significant correlation, and **c** for optimised LCI,

parameters **a** and **b** applied to flow accumulation and inverse distance to the stream/ditch **d**. relative weight of the top 5 % of weighted pixels. Grey areas represent low-flow periods, when two or more sampled streams were dry

Spatial aggregations of the LCI-TP

The LCI optimized for TP assigned nearly all of the weights (95%) to small areas (5%). Most of these areas were located near streams and ditches, but their width varied (Fig. 5a). The CSAs often extended ca. 100 m or more into agricultural areas, especially on long and convex hillslopes. Using LCI-TP values at the pixel level, we calculated $\text{LCI-TP}_{\text{field}}$ as the mean LCI-TP of each agricultural field. The $\text{LCI-TP}_{\text{field}}$ (Fig. 5b) revealed that most fields were weak sources of P (i.e. $\text{LCI-TP}_{\text{field}} \ll 1$), whereas a few fields were CSAs, as their $\text{LCI-TP}_{\text{field}}$ exceeded 10 and even 40. The associated histogram (Fig. 5c) followed a lognormal distribution, which confirms the high variability at the field scale (5th percentile-95th percentile, $q_5-q_{95} = 2.02e-03-1.40e+01$, $SD = 38.41$). When the LCI-TP was aggregated into 1 km^2 subcatchments ($\text{LCI-TP}_{1\text{km}^2}$) (Fig. 5d), its variability decreased drastically (Fig. 5f, min-max = 0–5.79, $SD = 0.71$). The number of subcatchments with $\text{LCI-TP}_{1\text{km}^2} > 1$ was

approximately the same as the number of subcatchments with $\text{LCI-TP}_{1\text{km}^2} < 1$ (Fig. 5f, median = 0.87), but the distribution remained lognormal. Following the same pattern, the LCI-TP aggregated into 25 km^2 subcatchments ($\text{LCI-TP}_{25\text{km}^2}$) had even lower variability (min-max = 0.64–1.44, $SD = 0.26$): at this scale the distribution was symmetrical (normal), and no subcatchment could be considered a CSA. The information at the subfield scale (Fig. 5a) and field scale (Fig. 5b), which is relevant for farmers and catchment managers, was generated for the entire study area (<https://antoine-csqn.github.io/YV1.html>).

Homogenisation of the LCI-TP with increasing catchment size

We delineated 500 subcatchments within the study area based on 500 points randomly generated over the hydrographic network. For each subcatchment, we calculated the LCI-TP (i.e. the LCI for $a = 1.4$ and

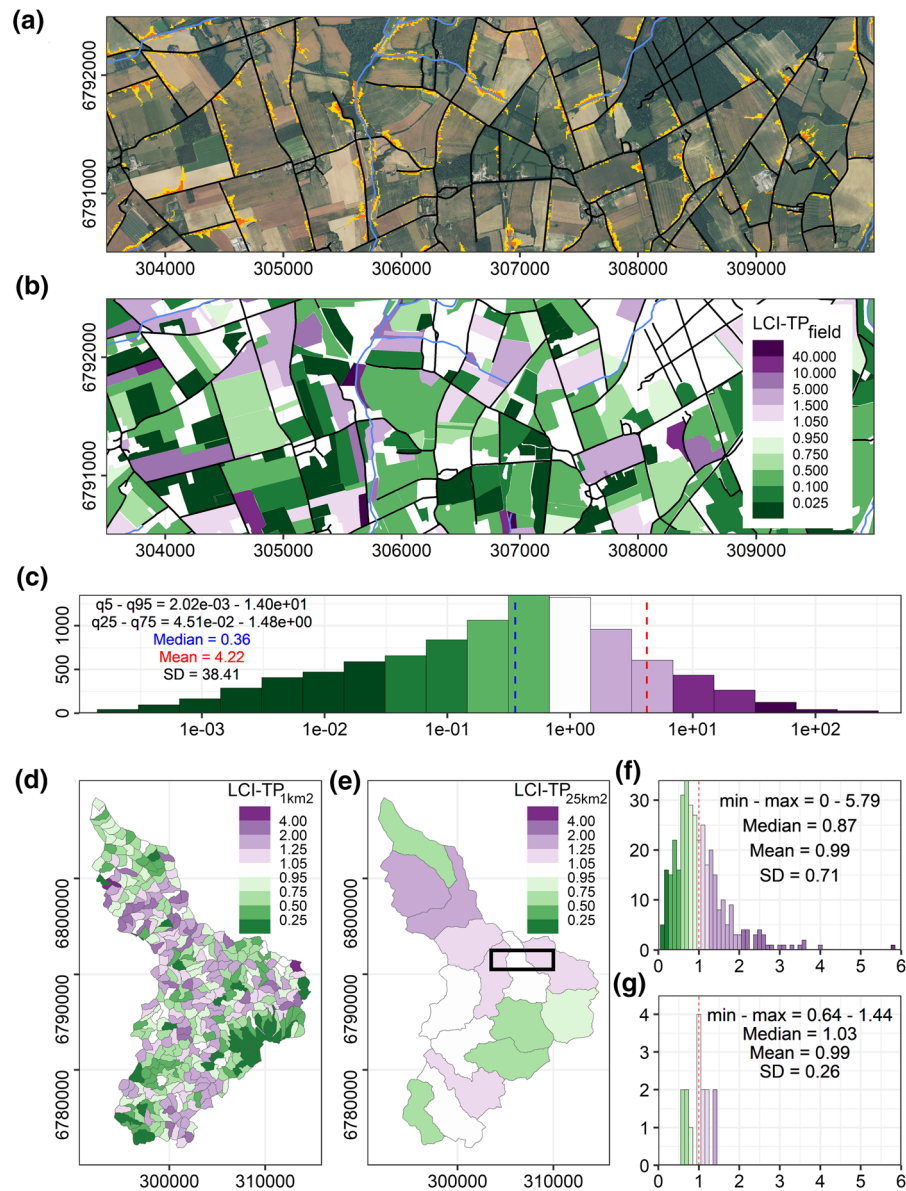


Fig. 5 **a** Excerpt of the study area, (refer to black rectangle in **e** for localisation) ca. 6 km × 2 km: top 5% (yellow) and 1% (red) of weighted pixels according to LCI-TP, **b** LCI-TP aggregated at the field scale (LCI-TP_{field}), and **c** histogram of

LCI-TP_{field} values for the whole study area (note the log scale on the x-axis). **d** LCI-TP for 1 km² subcatchments (LCI-TP_{1km²}) and **e** 25 km² subcatchments (LCI-TP_{25km²}) and associated histograms (**f** and **g**), respectively

$b = 2.2$), the landscape composition index (i.e. the LCI for $a = b = 0$), and their ratio, which we examined as a function of subcatchment area (Fig. 6).

This ratio varied greatly (0.02–3.37) for subcatchments smaller than 10 km², the typical size of 1st or 2nd order stream catchments but varied less (0.55–1.53) for subcatchments of 10–50 km². The high variability in this ratio, even for heavily farmed

subcatchments, indicates that the landscape configuration can be re-organised to limit TP exports. For catchments larger than 50 km², which corresponds to 4th order rivers in the study area, the ratio converged to 1. The main implication is that for headwater catchments (< 50 km²) the correlation between landscape composition and configuration (as defined by the LCI-TP) was weak and non-significant (Fig. S1),

while for larger catchments the correlation was strong (R^2 near 1) (Fig. S1).

Discussion

Spatial configuration of nutrient sources influences P but not N exports

In agricultural intensive landscapes, median NO_3^- concentrations are a proxy of N exports as spatial patterns of concentration are persistent through time (Gu et al. 2021) and NO_3^- represents most of the total N in streams (Dupas et al. 2015). Similarly, median TP concentrations are a proxy of P exports (Gu et al. 2021). Landscape composition is a strong predictor of N exports, while landscape configuration as defined here, appears to have no influence (Fig. 2a). This result agrees with previous research that indicates a strong correlation between metrics of agricultural N pressure, such as land use or the N surplus, and N concentrations in streams (Kronvang et al. 2005; Dupas et al. 2015), leaving little space for other controlling factors, such as the landscape configuration. However, distributed process-based modelling of N fate in agricultural catchments has shown that landscape configuration can have a small influence on N concentrations (Beaujouan et al. 2002; McDowell et al. 2014; Casal et al. 2019), which may not have been captured in our study. P concentrations are not related to landscape composition (Bol et al. 2018) or even P inputs (Dupas et al. 2015; Frei et al. 2020) in

headwater catchments. Multiple factors influence P transfers to streams: soil type and P content (Djordjic et al. 2004), tile-drainage (King et al. 2015a; King et al. 2015b), small ponds and hillside storage reservoirs (Schmadel et al. 2019), in-hillslope depressions (Smith and Livingston 2013), leaks from septic tanks (Withers et al. 2011) and livestock buildings, bank erosion (Kronvang et al. 2012), and ditch-dredging management (Smith and Pappas 2007). Without considering any of these factors, our optimised LCI ranked the headwater catchments reasonably well according to their P exports (Fig. 3b), although the residuals may be explained by these other factors. We demonstrate that the spatial configuration of P sources in the landscape is critical to understand P transfer from land to streams in headwater catchments. This influence of landscape configuration for TP but not NO_3^- is consistent with knowledge on their transfer pathways: TP is mainly transferred by surface flowpaths and can therefore be intercepted by landscape buffer zones, while NO_3^- is mainly transferred by deeper flowpaths and can therefore by-pass shallow retention hotspots (Strohmenger et al. 2020). The influence of the spatial configuration of nutrient sources on P but not N concentrations in agricultural headwater streams results in high variability in N:P ratios in these ecosystems. This variability affects stream algae communities, particularly their biomasses and the relative abundances of different taxa (Pringle 1990; Stelzer and Lamberti 2001).

The observation that landscape spatial organisation influences N and P transfers is not new. Nonetheless,

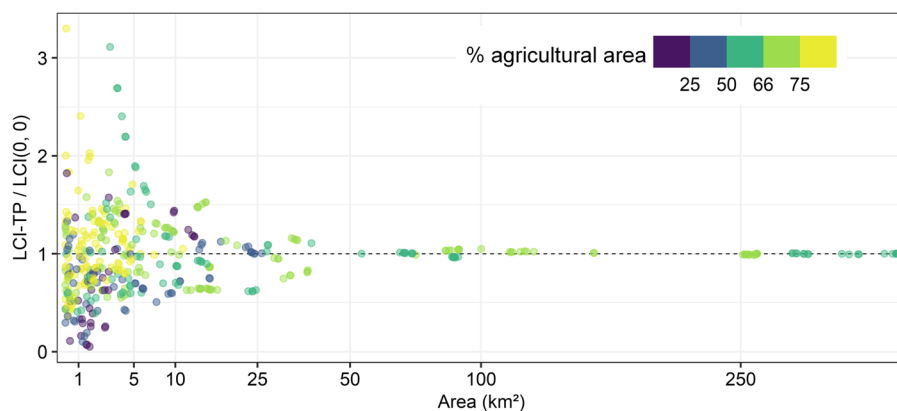


Fig. 6 Ratio of the LCI-TP (LCI for $a = 1.4$ and $b = 2.2$) to landscape composition index (LCI for $a = b = 0$) as a function of area (square-root-transformed x-axis) for 500 random

subcatchments in the study area (points). The colour indicates the percentage of agricultural land-use in each subcatchment

our approach differs from previous studies that used single or multiple regression of several landscape metrics, for example compiled in the FRAGSTATS software (McGarigal and Marks 1995), to predict nutrient exports at the catchment scale. Despite the large body of studies that use these landscape metrics (Lee et al. 2009; Bu et al. 2014; Ouyang et al. 2014; Zhang et al. 2019), several of the relationships do not have clear physical meaning, and the significant relationships differ among studies (Wang et al. 2020). We consider that these studies, taken together, are not conclusive for three reasons: (i) the large number of pairwise or multiple regressions between water quality parameters and landscape metrics increases the risk of generating spurious correlations (potential ecology fallacies), (ii) landscape metrics depend greatly on the resolution of GIS input data, and (iii) the studies do not consider the topological dimension, which is fundamental for explaining hillslope-to-stream transfers and landscape configuration (Thomas et al. 2016b). Several approaches have integrated this topological control with the hypothesis that nutrient sources near streams (Sliva and Dudley Williams 2001; Yates et al. 2014) and/or that overlap flow accumulation areas (Peterson et al. 2011; Staponites et al. 2019) have a disproportionately higher influence on nutrient exports than other areas. While these approaches still depend on the spatial resolution of GIS data, they are “hypothesis-driven” rather than purely “data-driven”, which decreases the risk of spurious correlations. A longstanding weakness of these approaches, however, is their rigidity due to the lack of calibrated parameters. For example, the HAI_{FLS} index (Peterson et al. 2011) and Flow-A index (Staponites et al. 2019) included both the distance to streams and flow accumulation, but the latter dominates the index value by construction, because it varies more than the former, and neither index allows both factors to be weighted by calibrated coefficients. The stochastic approach in the LCI developed here is more flexible, and we show that both hydrological distance and flow accumulation influence P transfer.

Spatial variability and temporal stability of critical source areas

One of the strongest correlation between median NO_3^- concentrations and LCI was for $(a, b) = (0, 0)$, which

shows that each source (agricultural area) contributed the same, regardless of its distance to streams or overlap with flow accumulation areas. This confirms the need to consider the entire catchment to reduce N loads in agricultural catchments. For median TP concentrations, the optimal was found for $(a, b) = (1.4, 2.2)$, a value for which 5% of the agricultural area contributed 95 % of the weight assigned by our index at the 10 m-pixel resolution. These values are similar to those found by Thomas et al. (2016a), who classified 1.6–3.4% of the catchment area (during median storm events) and 2.9–8.5% (during upper-quartile events) as prone to P transfer, based on a CSA model that also considered land use and topography as input variables. Summing the LCI-TP at the field scale indicates that the 20% of fields at highest risk represent 85% of the total weights, which are the fields on which mitigation measures should be prioritised. The distribution is asymmetrical, with 69% of fields having a mean $\text{LCI-TP}_{\text{field}}$ less than 1. This information at multiple scales can be a tool to maximise ecosystem services at the catchment scale, by reorganising landscapes to decrease P transfer without increasing the percentage of set-aside areas (Doody et al. 2016).

The shape and location of the sub-field CSAs overlap both the mandatory riparian buffer strips [5 m according to local application of the European Union Nitrate Directive (DREAL 2018)] and in-hillslope CSAs based on the Topographical Wetness Index (e.g. Page et al. 2005). Because most buffer strips in the study area were installed recently, we included them in P sources as they were enriched in P before conversion (Roberts et al. 2012; Dodd and Sharpley 2016; Jarvie et al. 2017; Gu et al. 2017; 2018). The location and shape of the CSAs indicate the need for new shapes of buffer zones, with variable widths and locations along ditches as well. Because buffer strips are critical sources of nutrients at the headwater catchment scale, they require new management practices. Potential solutions include sowing species that can capture more P (Roberts et al. 2020), mowing and exporting the residues each year (Fiorellino et al. 2017), and applying amendments that have high P-sorbing ability (Borno et al. 2018).

The temporal stability of the optimal parameters (a, b) for TP during the flow period is consistent with the spatial stability concept (Abbott et al. 2018), but is contrary to the concept of variable source areas (Collick et al. 2015; Dahlke et al. 2012). Our

interpretation of this temporal stability is that even though the soil-to-stream connectivity varied temporally during the sampling period, the TP concentrations observed may reflect the remobilisation of sediments transferred during rare erosion events. Observing storm events that result in surface transfers requires frequent observations (Cassidy and Jordan 2011). During the low-flow dates, the correlations with LCI-TP were not significant: different sources and sinks likely dominate the influence of agricultural areas and their configuration, which predominates during the flow period. Leaks from septic tanks or animal buildings and desorption from sediments are the most likely sources of P during this ecologically sensitive period, while hydrological disconnection, uptake, and sedimentation can be sinks of P (Lannergård et al. 2020; Sandstrom et al. 2020).

Landscape homogenisation with increasing catchment size: consequences for management, monitoring, and modelling

When LCI were aggregated into 1 km² subcatchments, which is the typical size of a 1st order catchment in the study area, the LCI-TP showed high spatial variability (Fig. 5d, f). This spatial variability decreased as the aggregation size increased (Fig. 5e, g), and landscape composition was weakly correlated with landscape configuration for catchments smaller than 50 km² but strongly correlated for those larger than 50 km² (Figs. S1, 6). These results explain, at least partially, why relationships between water quality parameters and landscape composition metrics break down below a certain catchment size (Bol et al. 2018). They also shed light on the long-standing difficulty in upscaling from nutrient export models at the field scale to those at the catchment scale: the spatial configuration of the nutrient sources can be critical.

The variability in the LCI-TP in small subcatchments and its homogenisation in larger catchments is the expression of a degree of unstructured heterogeneity (i.e. randomness) of the spatial configuration of agricultural areas (Musolff et al. 2017). Some almost entirely agricultural subcatchments have a LCI-TP less than 1, while some mixed-land-use catchments have a LCI-TP greater than 1. The latter provides the opportunity to introduce structured heterogeneity, i.e. to reorganise agricultural activities

spatially to reduce P transfers to streams (Musolff et al. 2017).

These results have implications for both modelling and monitoring. Semi-distributed models that simulate P exports from an entire catchment with simulation units smaller than 50 km² should include a coefficient to represent the spatial configuration of the agricultural areas. A distributed model should also consider ditches (as they are the entry point of P into the hydrographic network) and, especially, the spatial variability in P sources. When monitoring subcatchments that are smaller than the homogenisation threshold and have similar agricultural land-use composition, the observed differences in P loads cannot be related directly to the agricultural practices or soil properties. The spatial configuration of agricultural areas appears to exert a major control on median P concentrations. This is particularly important for targeting measures to the most cost-effective fields (Doody et al. 2016) and could increase in importance due to the recent development of innovative financial tools to improve water quality, such as payment for ecosystem services schemes, whose obligation to achieve results is increasing (Hejnowicz et al. 2014). Our research provides a data-driven method to identify CSAs and thus the most cost-effective fields on which to implement mitigation measures.

The 50 km² landscape homogenisation threshold found in this study is similar to the 18–68 km² stream-concentration thresholds found by Abbott et al. (2018) for the Rance and Haut-Couesnon catchments, also located in western France. We assume that the optimised coefficients and homogenisation threshold would vary with the topo-climatic conditions and agricultural landscape characteristics. More research is needed to confirm this connection between landscape configuration and P loads in different environmental settings. Given the high heterogeneity of landscape configuration below the 50 km² threshold, this research calls for a spatially dense monitoring network of headwater catchments. Monitoring catchments smaller than this homogenisation threshold allow the identification of critical source headwaters, where targeted action could be implemented. We also recommend using the LCI to investigate the influence of landscape configuration on other water contaminants that are transferred mainly by surface flow paths, such as some pesticides and faecal bacteria.

Author contributions AC: Conceptualization, Methodology, Formal analysis, Visualization, Writing - original draft. RD: Conceptualization, Supervision, Funding acquisition. SG: Sample collection and analysis. EC: Sample collection and analysis. GG: Project administration, Funding acquisition. PD: Supervision. All authors contributed substantially to revisions.

Funding The authors were supported by the Interreg project Channel Payments for Ecosystem Services, funded through the European Regional Development Fund (ERDF).

Data availability This study is based on a recently published dataset entitled *Repeated synoptic sampling for water chemistry monitoring in the Yvel catchment, northwestern France* available at <https://www.hydroshare.org/resource/7c7d7f6dd1f14450883ae1c243c3c28f/> (Dupas et al. 2020). It contains the hydrochemical data and the geographic information of the study site.

Code availability The code (R script) produced to analyse the data and produce the Figures is available at <https://github.com/Antoine-CSQN/landscape-configuration-paper>.

Declarations

Conflict of interest The authors declare that they have no known competing financial interests or personal relationships that could have appeared to influence the work reported in this paper.

Consent for publication All co-authors—A. Casquin, R. Dupas, S. Gu, E. Couic, G. Gruau and P. Durand—have approved the manuscript and agree with its submission to Landscape Ecology.

References

- Abbott BW, Gruau G, Zarnetske JP, Moatar F, Barbe L, Thomas Z, Fovet O, Kolbe T, Gu S, Pierson-Wickmann AC, Davy P (2018) Unexpected spatial stability of water chemistry in headwater stream networks. *Ecol Lett* 21:296–308
- Ahiablame LM, Chaubey I, Smith DR, Engel BA (2011) Effect of tile effluent on nutrient concentration and retention efficiency in agricultural drainage ditches. *Agric Water Manag* 98:1271–1279
- Beaujouan V, Durand P, Ruiz L, Arousseau P, Cotteret G (2002) A hydrological model dedicated to topography-based simulation of nitrogen transfer and transformation: rationale and application to the geomorphology-denitrification relationship. *Hydrological Processes* 16:493–507
- Bishop K, Buffam I, Erlandsson M, Fölster J, Laudon H, Seibert J, Temnerud J (2008) Aqua Incognita: the unknown headwaters. *Hydrol Process* 22:1239–1242
- Bol R, Gruau G, Mellander PE, Dupas R, Bechmann M, Skarbøvik E, Bierzoza M, Djodjic F, Glendell M, Jordan P, Van der Grift B (2018) Challenges of reducing phosphorus based water eutrophication in the agricultural landscapes of Northwest Europe. *Front Mar Sci*. <https://doi.org/10.3389/fmars.2018.00276>
- Borno ML, Muller-Stover DS, Liu F (2018) Contrasting effects of biochar on phosphorus dynamics and bioavailability in different soil types. *Sci Total Environ* 627:963–974
- Bu H, Meng W, Zhang Y, Wan J (2014) Relationships between land use patterns and water quality in the Taizi River basin, China. *Ecol Indic* 41:187–197
- Buchanan B, Easton ZM, Schneider RL, Walter MT (2013) Modeling the hydrologic effects of roadside ditch networks on receiving waters. *J Hydrol* 486:293–305
- Buchanan BP, Archibald JA, Easton ZM, Shaw SB, Schneider RL, Walter MT (2013) A phosphorus index that combines critical source areas and transport pathways using a travel time approach. *J Hydrol* 486:123–135
- Burt TP, Pinay G (2005) Linking hydrology and biogeochemistry in complex landscapes. *Prog Phys Geogr* 29:297–316
- Casal L, Durand P, Akkal-Corfini N, Benhamou C, Laurent F, Salmon-Monviola J, Vertès F (2019) Optimal location of set-aside areas to reduce nitrogen pollution: a modelling study. *J Agric Sci* 156:1090–1102
- Casquin A, Gu S, Dupas R, Petitjean P, Gruau G, Durand P (2020) River network alteration of C-N-P dynamics in a mesoscale agricultural catchment. *Sci Total Environ* 749:141551
- Cassidy R, Jordan P (2011) Limitations of instantaneous water quality sampling in surface-water catchments: comparison with near-continuous phosphorus time-series data. *J Hydrol* 405:182–193
- Cole LJ, Stockan J, Helliwell R (2020) Managing riparian buffer strips to optimise ecosystem services: a review. *Agric Ecosyst Environ*. <https://doi.org/10.1016/j.agee.2020.106891>
- Collick AS, Fuka DR, Kleinman PJ, Buda AR, Weld JL, White MJ, Veith TL, Bryant RB, Bolster CH, Easton ZM (2015) Predicting phosphorus dynamics in complex terrains using a variable source area hydrology model. *Hydrol Process* 29:588–601
- Collins AL, Zhang Y, McChesney D, Walling DE, Haley SM, Smith P (2012) Sediment source tracing in a lowland agricultural catchment in southern England using a modified procedure combining statistical analysis and numerical modelling. *Sci Total Environ* 414:301–317
- Dahlke HE, Easton ZM, Lyon SW, Todd Walter M, Destouni G, Steenhuis TS (2012) Dissecting the variable source area concept – subsurface flow pathways and water mixing processes in a hillslope. *J Hydrol* 420–421:125–141
- Djodjic F, Borling K, Bergstrom L (2004) Phosphorus leaching in relation to soil type and soil phosphorus content. *J Environ Qual* 33:678–684
- Dodd RJ, Sharpley AN (2016) Conservation practice effectiveness and adoption: unintended consequences and implications for sustainable phosphorus management. *Nutr Cycl Agroecosyst* 104:373–392
- Dodds W, Smith V (2016) Nitrogen, phosphorus, and eutrophication in streams. *Inland Waters* 6:155–164
- Dodds WK, Oakes RM (2008) Headwater influences on downstream water quality. *Environ Manag* 41:367–377
- Doody DG, Archbold M, Foy RH, Flynn R (2012) Approaches to the implementation of the water framework directive: targeting mitigation measures at critical source areas of

- diffuse phosphorus in Irish catchments. *J Environ Manag* 93:225–234
- Doody DG, Withers PJ, Dils RM, McDowell RW, Smith V, McElarney YR, Dunbar M, Daly D (2016) Optimizing land use for the delivery of catchment ecosystem services. *Front Ecol Environ* 14:325–332
- Downing J (2012) Global abundance and size distribution of streams and rivers. *Inland Waters* 2:229–236
- DREAL B (2018) Directive nitrates 5ème programme d'actions en Bretagne. <http://www.bretagne.developpement-durable.gouv.fr/cinquieme-programme-d-actions-regional-directive-r837.html>. Accessed 11 January 2021
- Dunne EJ, Mckee KA, Clark MW, Grunwald S, Reddy KR (2007) Phosphorus in agricultural ditch soil and potential implications for water quality. *J Soil Water Conserv* 62:244–252
- Dupas R, Delmas M, Dorioz J-M, Garnier J, Moatar F, Gascuel-Odoux C (2015) Assessing the impact of agricultural pressures on N and P loads and eutrophication risk. *Ecol Ind* 48:396–407
- Dupas R, Minaudo C, Abbott BW (2019) Stability of spatial patterns in water chemistry across temperate ecoregions. *Environ Res Lett* 14:074015
- Dupas R, Gu S, Casquin A, Gruau G, Petitjean P, Durand P (2020) Repeated synoptic sampling for water chemistry monitoring in the Yvel catchment, northwestern France Hydroshare. <http://www.hydroshare.org/resource/7c7d7f6dd1f14450883ae1c243c3c28f>
- Fiorellino N, Kratochvil R, Coale F (2017) Long-term agronomic drawdown of soil phosphorus in Mid-Atlantic coastal plain. *Soils Agron J* 109:455–461
- Frei RJ, Abbott BW, Dupas R, Gu S, Gruau G, Thomas Z, Kolbe T, Aquilina L, Labasque T, Laverman A, Fovet O (2020) Predicting nutrient incontinence in the anthropocene at watershed scales. *Front Environ Sci*. <https://doi.org/10.3389/fenvs.2019.00200>
- Gburek WJ, Sharpley AN (1998) Hydrologic controls on phosphorus loss from upland agricultural watersheds. *J Environ Qual* 27:267–277
- Giri S, Qiu Z, Zhang Z (2018) Assessing the impacts of land use on downstream water quality using a hydrologically sensitive area concept. *J Environ Manag* 213:309–319
- Goyette J-O, Bennett EM, Maranger R (2018) Differential influence of landscape features and climate on nitrogen and phosphorus transport throughout the watershed. *Biogeochemistry* 142:155–174
- Gu S, Gruau G, Dupas R, Rumpel C, Crème A, Fovet O, Gascuel-Odoux C, Jeanneau L, Humbert G, Petitjean P (2017) Release of dissolved phosphorus from riparian wetlands: evidence for complex interactions among hydroclimate variability, topography and soil properties. *Sci Total Environ* 598:421–431
- Gu S, Gruau G, Malique F, Dupas R, Petitjean P, Gascuel-Odoux C (2018) Drying/rewetting cycles stimulate release of colloidal-bound phosphorus in riparian soils. *Geoderma* 321:32–41
- Gu S, Casquin A, Dupas R, Abbott BW, Petitjean P, Durand P, Gruau G (2021) Spatial persistence of water chemistry patterns across flow conditions in a mesoscale agricultural catchment. *Water Resour Res*. <https://doi.org/10.1029/2020WR029053>
- Hashemi F, Olesen JE, Hansen AL, Borgesen CD, Dalgaard T (2018) Spatially differentiated strategies for reducing nitrate loads from agriculture in two Danish catchments. *J Environ Manag* 208:77–91
- Hejnowicz AP, Raffaelli DG, Rudd MA, White PCL (2014) Evaluating the outcomes of payments for ecosystem services programmes using a capital asset framework. *Ecosyst Serv* 9:83–97
- Hill CR, Robinson JS (2012) Phosphorus flux from wetland ditch sediments. *Sci Total Environ* 437:315–322
- IGN (2018) RGE ALTI version 2.0 Les modèles numériques 3D. https://geoservices.ign.fr/ressources_documentaires/Espace_documentaire/MODELES_3D/RGE_ALTI/DL_RGEALTI_2-0.pdf. Accessed 11 January 2021
- Jarvie HP, Johnson LT, Sharpley AN, Smith DR, Baker DB, Bruulsema TW, Confesor R (2017) Increased soluble phosphorus loads to Lake Erie: unintended consequences of conservation practices? *J Environ Qual* 46:123–132
- King KW, Williams MR, Fausey NR (2015) Contributions of systematic tile drainage to watershed-scale phosphorus transport. *J Environ Qual* 44:486–494
- King KW, Williams MR, Macrae ML, Fausey NR, Frankenberg J, Smith DR, Kleinman PJ, Brown LC (2015) Phosphorus transport in agricultural subsurface drainage: a review. *J Environ Qual* 44:467–485
- Kronvang B, Audet J, Baattrup-Pedersen A, Jensen HS, Larsen SE (2012) Phosphorus load to surface water from bank erosion in a Danish lowland river basin. *J Environ Qual* 41:304–313
- Kronvang B, Jeppesen E, Conley DJ, Søndergaard M, Larsen SE, Ovesen NB, Carstensen J (2005) Nutrient pressures and ecological responses to nutrient loading reductions in Danish streams, lakes and coastal waters. *J Hydrol* 304:274–288
- Lannergård EE, Agstam-Norlin O, Huser BJ, Sandström S, Rakovic J, Futter MN (2020) New insights into legacy phosphorus from fractionation of streambed sediment. *J Geophys Res*. <https://doi.org/10.1029/2020jg005763>
- Le Moal M, Gascuel-Odoux C, Ménesguen A, Souchon Y, Étrillard C, Levain A, Moatar F, Pannard A, Souchu P, Lefebvre A, Pinay G (2018) Eutrophication: a new wine in an old bottle? *Sci Total Environ* 651:1–11
- Lee S-W, Hwang S-J, Lee S-B, Hwang H-S, Sung H-C (2009) Landscape ecological approach to the relationships of land use patterns in watersheds to water quality characteristics. *Landsc Urban Plan* 92:80–89
- Levavasseur F, Martin P, Bouty C, Barbottin A, Bretagnolle V, Théron O, Scheurer O, Piskiewicz N (2016) RPG explorer: a new tool to ease the analysis of agricultural landscape dynamics with the land parcel identification system. *Comput Electron Agric* 127:541–552
- Lintern A, Webb JA, Ryu D, Liu S, Bende-Michl U, Waters D, Leahy P, Wilson P, Western AW (2018) Key factors influencing differences in stream water quality across space. *Wiley Interdiscip Rev*. <https://doi.org/10.1002/wat2.1260>
- Liu J, Liu X, Wang Y, Li Y, Jiang Y, Fu Y, Wu J (2020) Landscape composition or configuration: which contributes more to catchment hydrological flows and variations? *Landsc Ecol* 35:1531–1551

- McDowell RW, Moreau P, Salmon-Monviola J, Durand P, Leterme P, Merot P (2014) Contrasting the spatial management of nitrogen and phosphorus for improved water quality: modelling studies in New Zealand and France. *European J Agron* 57:52–61
- McDowell RW, Srinivasan MS (2009) Identifying critical source areas for water quality: 2. Validating the approach for phosphorus and sediment losses in grazed headwater catchments. *J Hydrol* 379:68–80
- McGarigal K, Marks BJ (1995) FRAGSTATS: spatial pattern analysis program for quantifying landscape structure. US Department of Agriculture, Forest Service, Pacific Northwest Research Station, Corvallis
- Moatar F, Floury M, Gold AJ, Meybeck M, Renard B, Ferréol M, Chandresris A, Minaudo C, Addy K, Piffady J, Pinay G (2020) Stream solutes and particulates export regimes: a new framework to optimize their monitoring. *Front Ecol Evol*. <https://doi.org/10.3389/fevo.2019.00516>
- Murphy J, Riley JP (1962) A modified single solution method for the determination of phosphate in natural waters. *Anal Chim Acta* 27:31–36
- Musolff A, Fleckenstein JH, Rao PSC, Jawitz JW (2017) Emergent archetype patterns of coupled hydrologic and biogeochemical responses in catchments. *Geophys Res Lett* 44:4143–4151
- O'Callaghan JF, Mark DM (1984) The extraction of drainage networks from digital elevation data. *Computer Vision. Graph Image Process* 28:323–344
- ODEM (2012) Apports de phosphore et proliférations de cyanobactéries dans le Lac au Duc (Morbihan)
- Ouyang W, Song K, Wang X, Hao F (2014) Non-point source pollution dynamics under long-term agricultural development and relationship with landscape dynamics. *Ecol Ind* 45:579–589
- Page T et al (2005) Spatial variability of soil phosphorus in relation to the topographic index and critical source areas: sampling for assessing risk to water quality. *J Environ Qual* 34:2263–2277
- Peterson EE, Sheldon F, Darnell R, Bunn SE, Harch BD (2011) A comparison of spatially explicit landscape representation methods and their relationship to stream condition. *Freshw Biol* 56:590–610
- Pionke HB, Gburek WJ, Sharpley AN (2000) Critical source area controls on water quality in an agricultural watershed located in the Chesapeake Basin. *Ecol Eng* 14:325–335
- Planchon O, Darboux F (2002) A fast, simple and versatile algorithm to fill the depressions of digital elevation models. *Catena* 46:159–176
- Pringle CM (1990) Nutrient spatial heterogeneity: effects on community structure physiognomy diversity of stream algae. *Ecology* 71:905–920
- Qin C, Zhu AX, Pei T, Li B, Zhou C, Yang L (2007) An adaptive approach to selecting a flow-partition exponent for a multiple-flow-direction algorithm. *Int J Geogr Inf Sci* 21:443–458
- Reaney SM, Mackay EB, Haygarth PM, Fisher M, Molineux A, Potts M, Benskin CMH (2019) Identifying critical source areas using multiple methods for effective diffuse pollution mitigation. *J Environ Manag* 250:109366
- Roberts WM, Stutter MI, Haygarth PM (2012) Phosphorus retention and remobilization in vegetated buffer strips: a review. *J Environ Qual* 41:389–399
- Roberts WM, George TS, Stutter MI, Louro A, Ali M, Haygarth PM (2020) Phosphorus leaching from riparian soils with differing management histories under three grass species. *J Environ Qual* 49:74–84
- Sandstrom S, Futter MN, Kyllmar K, Bishop K, O'Connell DW, Djodjic F (2020) Particulate phosphorus and suspended solids losses from small agricultural catchments: links to stream and catchment characteristics. *Sci Total Environ* 711:134616
- Schmadel NM, Harvey JW, Schwarz GE, Alexander RB, Gomez-Velez JD, Scott D, Ator SW (2019) Small ponds in headwater catchments are a dominant influence on regional nutrient and sediment budgets. *Geophys Res Lett* 46:9669–9677
- Sharpley AN, Kleinman PJA, Flaten DN, Buda AR (2011) Critical source area management of agricultural phosphorus: experiences, challenges and opportunities. *Water Sci Technol* 64:945–952
- Shatwell T, Köhler J (2018) Decreased nitrogen loading controls summer cyanobacterial blooms without promoting nitrogen-fixing taxa: Long-term response of a shallow lake. *Limnol Oceanogr*. <https://doi.org/10.1002/lno.11002>
- Shi ZH, Ai L, Li X, Huang XD, Wu GL, Liao W (2013) Partial least-squares regression for linking land-cover patterns to soil erosion and sediment yield in watersheds. *J Hydrol* 498:165–176
- Shore M, Jordan P, Mellander PE, Kelly-Quinn M, Wall DP, Murphy PN, Melland AR (2014) Evaluating the critical source area concept of phosphorus loss from soils to waterbodies in agricultural catchments. *Sci Total Environ* 490:405–415
- Sliva L, Dudley Williams D (2001) Buffer zone versus whole catchment approaches to studying land use impact on river water quality. *Water Res* 35:3462–3472
- Smith DR (2009) Assessment of in-stream phosphorus dynamics in agricultural drainage ditches. *Sci Total Environ* 407:3883–3889
- Smith DR, Livingston SJ (2013) Managing farmed closed depressional areas using blind inlets to minimize phosphorus and nitrogen losses. *Soil Use Manag* 29:94–102
- Smith DR, Pappas EA (2007) Effect of ditch dredging on the fate of nutrients in deep drainage ditches of the Midwestern United States. *J Soil Water Conserv* 62:252–261
- Srinivasan MS, McDowell RW (2009) Identifying critical source areas for water quality: 1. Mapping and validating transport areas in three headwater catchments in Otago, New Zealand. *J Hydrol* 379:54–67
- Staponites LR, Bartak V, Bily M, Simon OP (2019) Performance of landscape composition metrics for predicting water quality in headwater catchments. *Sci Rep* 9:14405
- Steffen W et al (2015) Sustainability. Planetary boundaries: guiding human development on a changing planet. *Science* 347:1259855
- Stelzer RS, Lamberti GA (2001) Effects of N: P ratio and total nutrient concentration on stream periphyton community structure, biomass, and elemental composition. *Limnol Oceanogr* 46:356–367

- Strohmeier L, Fovet O, Akkal-Corfini N, Dupas R, Durand P, Fauchoux M, Gruau G, Hamon Y, Jaffrézic A, Minaudo C, Petitjean P (2020) Multitemporal relationships between the hydroclimate and exports of carbon, nitrogen, and phosphorus in a small agricultural watershed. *Water Resour Res*. <https://doi.org/10.1029/2019wr026323>
- Temnerud J, Bishop K (2005) Spatial variation of streamwater chemistry in two Swedish boreal catchments: implications for environmental assessment. *Environ Sci Technol* 39:1463–1469
- Thomas IA, Mellander PE, Murphy PN, Fenton O, Shine O, Djodjic F, Dunlop P, Jordan P (2016) A sub-field scale critical source area index for legacy phosphorus management using high resolution data. *Agric Ecosyst Environ* 233:238–252
- Thomas Z, Abbott BW (2018) Hedgerows reduce nitrate flux at hillslope and catchment scales via root uptake and secondary effects. *J Contam Hydrol* 215:51–61
- Thomas Z, Abbott BW, Troccaz O, Baudry J, Pinay G (2016) Proximate and ultimate controls on carbon and nutrient dynamics of small agricultural catchments. *Biogeochemistry* 13:1863–1875
- Uuemaa E, Roosaare J, Mander Ü (2007) Landscape metrics as indicators of river water quality at catchment scale. *Hydrol Res* 38:125–138
- Wang M, Wang Y, Li Y, Liu X, Liu J, Wu J (2020) Natural and anthropogenic determinants of riverine phosphorus concentration and loading variability in subtropical agricultural catchments. *Agric Ecosyst Environ*. <https://doi.org/10.1016/j.agee.2019.106713>
- Withers P, Neal C, Jarvie H, Doody D (2014) Agriculture and eutrophication: where do we go from here? *Sustainability* 6:5853–5875
- Withers PJ, Jarvie HP, Stoate C (2011) Quantifying the impact of septic tank systems on eutrophication risk in rural headwaters. *Environ Int* 37:644–653
- Xiao R, Wang G, Zhang Q, Zhang Z (2016) Multi-scale analysis of relationship between landscape pattern and urban river water quality in different seasons. *Sci Rep* 6:25250
- Yates AG, Brua RB, Corriveau J, Culp JM, Chambers PA (2014) Seasonally driven variation in spatial relationships between agricultural land use and in-stream nutrient concentrations. *River Res Appl* 30:476–493
- Zhang W, Pueppke SG, Li H, Geng J, Diao Y, Hyndman DW (2019) Modeling phosphorus sources and transport in a headwater catchment with rapid agricultural expansion. *Environ Pollut*. <https://doi.org/10.1016/j.envpol.2019.113273>

Publisher's Note Springer Nature remains neutral with regard to jurisdictional claims in published maps and institutional affiliations.